System analysis of *Phycomyces* light-growth response: *madC*, *madG*, and *madH* mutants

Anuradha Palit,* Promod R. Pratap,‡ and Edward D. Lipson
Department of Physics, Syracuse University, Syracuse, New York 13244-1130; and Department of Pediatrics* and Physiology,‡ State University of New York Health Science Center, Syracuse, New York 13210

ABSTRACT The light-growth response of *Phycomyces* has been studied further with the sum-of-sinusoids method in the framework of the Wiener theory of nonlinear system identification. The response was treated as a black box with the logarithm of light intensity as the input and elongation rate as the output. The nonlinear input-output relation of the light-growth response can be represented mathematically by a set of weighting functions called kernels, which appear in the Wiener intergral series. The linear (first-order) kernels of wild type, and of single and double mutants affected in genes *madA* to *madG* were determined previously with Gaussian white noise test stimuli, and were used to investigate the interactions among the products of these genes (R. C. Poe, P. Pratap, and E. D. Lipson. 1986. *Biol. Cybern.* 55:105.). We have used the more precise sum-of-sinusoids method to extend the interaction studies, including both the first- and second-order kernels. Specifically, we have investigated interactions of the *madH* ("hypertropic") gene product with the *madC* ("night blind") and *madG* ("stiff") gene products. Experiments were performed on the *Phycomyces* tracking machine. The log-mean intensity of the stimulus was 6×10^{-2} W m^{-2} and the wavelength was 477 nm. The first- and second-order kernels were analyzed in terms of nonlinear kinetic models. The *madH* gene product was found to interact with those of *madC* and *madG*. This result extends previous findings that the *madH* gene product is associated with the input and the ouput of the sensory transduction complex for the light-growth response.

INTRODUCTION

The fungus *Phycomyces* shows numerous responses to blue light (Cerdá-Olmedo and Lipson, 1987). The light-growth response and phototropism of its sporangiophore, or fruiting body, are sensitive over a range of 10^{10}:1 in blue light intensity with an absolute threshold of 10^{-9} W m^{-2}. Analyses of behavioral mutants have revealed eight unlinked genes that affect the light responses of the sporangiophore (Cerdá-Olmedo and Lipson, 1987). The elongation rate of the sporangiophore varies transiently in response to changes in the light intensity. This light-growth response of the wild type and of "night-blind" and "stiff" mutants (see below) has been studied with classical stimuli (pulses, steps and sinusoids; by Foster and Lipson 1973) and with system identification and analysis methods (Marmarelis and Marmarelis, 1978; Victor and Shapley, 1980) employing Gaussian white noise stimuli (Lipson 1975*a–c*; Poe and Lipson, 1986; Poe et al., 1986*a*, *b*), and sum-of-sinusoids stimuli (Pratap et al., 1986*a*, *b*; Palit et al., 1986).

In these system analysis studies, the light-growth response has been treated as a black-box system with the logarithm of light intensity as input and the elongation rate as the output. The system is represented mathematically by a set of weighting functions called kernels. A nonlinear model was derived from the analysis of the first- and second-order frequency kernels for wild type (Pratap et al., 1986*a*). This model includes a nonlinear dynamic subsystem followed by a linear dynamic subsystem.

The white-noise method was used previously to probe the dynamic interactions among the products of seven games, *madA* to *madG*, and evaluate their organization in the sensory transduction pathway for the light-growth response (Poe et al., 1986*b*). Mutants defective in genes *madA* to *madC* are termed night blind because they have much higher thresholds than the wild type (reduced sensitivity). Mutants affected in genes *madD* through *madG* are called stiff because the show weak bending (and growth modulation) responses. The *madH* mutants are "hypertropic," in that they exhibit enhanced bending responses (viz. phototropism, avoidance, and gravitropism).

Here, we have investigated double mutants (López-Díaz and Lipson, 1983) carrying *madH* (hypertropic) mutations together with *madC* (night blind) or *madG* (stiff) mutations. The photogravitropism phenotypes (threshold curves, of double mutants with stiff and hypertropic mutations are intermediate between those of the parental single mutant strains (López-Díaz and Lipson, 1983); the opposing mutations roughly compensated each other, giving essentially wild-type behavior. The *madC madH* double mutants have the same elevated threshold

Correspondence and reprint requests to E. D. Lipson.

0006-3495/89/03/519/08 $2.00

for phototropism as *madC* mutants, but bend like hypertropic mutants in the region just above the threshold and at high intensity.

Recombinants were found after crosses between the *madG* (hereafter abbreviated as G) strain C288 and all seven hypertropic mutants; therefore, none of the hypertropic mutations occur in the G gene (López-Díaz and Lipson, 1983). The *madH* (H) and *madC* (C) genes were also shown by recombination analysis to be unlinked. However, C and H mutants do not complement. This result suggested an interaction between C and H gene products.

Instead of using the white-noise method to identify the system kernels (Poe et al., 1986*b*), we have adopted the more precise sum-of-sinusoids method (Pratap et al., 1986*a*). In the earlier work, which involved only genes A through G, interactions were determined on the basis of just the first-order kernels. Here, both the first- and second-order kernels have been used so that both linear and nonlinear interactions could be tested.

MATERIALS AND METHODS

Strains, culture conditions, tracking machine, and light source

The strains are listed in Table 1. Growth conditions were similar to those described previously (Pratap et al., 1986*a*; Poe and Lipson, 1986). Experiments were performed on the *Phycomyces* tracking machine (Foster and Lipson, 1973; Lipson 1975*a*). To begin each experiment, a vial containing a single sporangiophore was placed on the servo-controlled three-dimensional stage. The stage was moved continuously to keep the spherical sporangium fixed in space. The elongation rate of the sporangiophore was deduced from the vertical motion of the stage.

TABLE 1 Strains used in this work

Strain	Genotype*	Origin‡
NRRL1555	(−)	Wild-type
L15	*madC119 nicA101(−)*	C264 × C148
C288	*madG131(+)*	C107 × C264
L83	*madH703(−)*	NRRL1555, MNNG
L84	*madH704(−)*	NRRL1555, MNNG
L85	*madH705(−)*	NRRL1555, MNNG
L122	*madC119 madH705(+)*	L2 × L85
L115	*madG131 madH704(−)*	C288 × L84
L118	*madG131 madH703(−)*	C288 × L83

**mad* indicates abnormal phototropism: *nic* indicates a requirement for nicotinic acid. (−) and (+) denote mating types. The *mad* phenotypes are as follows: *madC* = night blind, *madG* = stiff, and *madH* = hypertropic (alleles *madH703* and *madH705* are recessive, and *madH704* is dominant; López-Díaz and Lipson, 1983).

‡MNNG indicates that these strains were isolated after treatment of NRRL1555 with the chemical mutagen N-Methyl-N'-nitro-N-nitroso-guanidine. The symbol × denotes a sexual cross.

The sporangiophore was enclosed within a temperature controlled chamber maintained at 20°C.

The stimulus light source was 500-W tungsten-halogen lamp (model 500Q/CL; GTE Sylvania, Inc., Salem, MA). The light from the lamp passed through a heat filter and a 477 nm interference filter (Balzers B-40, 9-12 nm bandwidth, Rolyn Optics, Covina, CA) and then was focused by lenses onto the common end of a bifurcated fiber-optic light guide (Valtec, Inc., West Boylston, MA). Just in front of the light guide was a 4.0 O.D. circular neutral density wedge, which was rotated under servo control by a microcomputer programmed to vary the stimulus light intensity with time (see below). The other two ends of the light guide directed the light symmetrically and bilaterally onto the growing zone of the sporangiophore at an angle of ~30° below the horizontal.

Stimulus

The stimulus was a sum of 15 sinusoids of equal amplitude. The frequencies of the sinusoidal components were multiples of a fundamental frequency 3.66×10^{-3} min^{-1} (inverse of the analyzed experimental duration of 273.1 min). The set of 15 frequency multipliers was {7, 17, 33, 53, 71, 80, 92, 115, 147, 192, 249, 297, 338, 380, and 473}. The stimulus log-mean intensity I_0 (defined by $\log I_0 = \langle \log I \rangle$, where the angle brackets represent a time average) was 6×10^{-2} W m^{-2} at a wavelength of 477 nm. The data were analyzed as described by Pratap et al. (1986*a*). The stimulus and the response were transformed to the frequency domain with a Fast Fourier Transform (FFT) algorithm (Stanley, 1975). The first- and second-order frequency kernels, H_1 and H_2 were obtained according to the following relations (Pratap et al., 1986*a*)

$$H_1(f) = \frac{R(f)}{S(f)} \tag{1}$$

$$H_2(f_1, f_2) = \frac{R(f_1 + f_2)}{S(f_1)\,S(f_2),} \tag{2}$$

where $S(f)$ and $R(f)$ are the Fourier transforms of the stimulus and response, and f, as well as f_1 and f_2, represent any of the component frequencies of the sum-of-sinusoids stimulus.

The experimentally-derived kernels together with the Wiener series (Marmarelis and Marmarelis, 1978; Victor and Shapley, 1980) constitute a nonparametric external model of the system (Pratap et al., 1986*a*). To interpret the external model, an analytical model based on the structure of the kernels was developed (Pratap et al., 1986*a*); this internal model, with adjustable parameters, was fit to the external model (i.e., the experimental kernels). The fits were carried out on the campus computer (IBM 4341) with nonlinear least-squares algorithms (Marquardt, 1963; Hamilton, 1964) in the computer language APL. The second-order internal model responses were calculated only for frequency pairs for which the combination frequency was <0.66 min^{-1}. This frequency was six times the system cutoff frequency for wild type (0.11 min^{-1}), defined as the frequency where the magnitude of the response has fallen to 70.7% of the maximum value. This procedure gave a total of 96 model points to be fit to the corresponding experimental points. This restriction on the number of points in the fit was necessary because of limitations in the APL workspace size. The points omitted from the fitting procedure was essentially zero, within errors.

The model for the wild-type light-growth response (Fig. 1) consists of a central linear subsystem composed of filters, preceded by a subsystem with a nonlinear feedforward path composed of linear dynamic elements and a static squarer (Pratap et al., 1986*a*). The linear subsystem consists of a cascade of two distinct second-order low-pass filters, a first-order high-pass filter, a gain factor, and a delay element (note: when we use

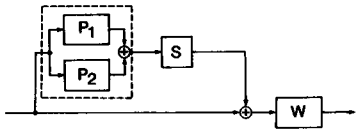

FIGURE 1 A generalized model with a dynamic second-order nonlinear subsystem towards the input. This configuration provides a good fit to the data for the wild type. P_1, P_2, and W are dynamic linear systems. S is a squarer. The first-order (linear) response is due just to W. The second-order (nonlinear) response is due to squarer S. P_1 and P_2 make the nonlinear path itself dynamic. P_1 is a second-order low-pass filter and P_2 is a high-pass filter (Eq. 4). W is a fifth-order linear system described by the analytical transfer function (Eq. 3)

the term order in referring to filters, we mean dynamic order, as opposed to the kernel order, which is associated with linear or nonlinear behavior):

$$W(s) = \beta_L e^{-st_0}\left[\frac{s}{s + 2\pi f_1}\right]\left[\frac{(2\pi f_2)^2}{s^2 + (2\alpha)(2\pi f_2)\, s + (2\pi f_2^2)}\right] \cdot \left[\frac{(2\pi f_2')^2}{s^2 + (2\alpha')(2\pi f_2')\, s + (2\pi f_2')^2}\right], \quad (3)$$

where s is the Laplace transform variable; β_L is the overall gain; t_0 is the latency; f_1 is the cutoff frequency of the high-pass filter; f_2 and f_2' are the cutoff frequencies of the low-pass filters; and α and α' are damping constants. The ordering of these linear elements is arbitrary.

The nonlinear subsystem includes a static squarer preceded by the sum of two linear filters (a low-pass filter P_1 and a high-pass filter P_2; Eq. 4).

$$P_1(s) = \frac{\beta_{N1}}{[s^2 + (2\alpha_{N1})(2\pi f_{N1})\, s + (2\pi f_{N1})^2]}$$
$$P_2(s) = \frac{\beta_{N2} s}{[s^2 + (2\alpha_{N2})(2\pi f_{N2})\, s + (2\pi f_{N2})^2]^n}, \quad (4)$$

where b_{N1}, f_{N1}, and α_{N1} are respectively the gain, the cutoff frequency and the damping constant of the low-pass filter and β_{N2}, f_{N2}, α_{N2} and n are respectively the gain, the cutoff frequency, damping constant and the exponent of the high-pass filter.

RESULTS

Fig. 2 shows the magnitude (absolute value) of the first-order frequency kernels. The curves represent a nonlinear least-squares fit of the linear model (Eq. 3) to the complex-valued first-order kernels. For wild type and most of the mutants, the curves at low frequencies rise in direct proportion to the frequency like a first-order high-pass filter; such behavior has been previously associated with adaptation (Lipson, 1975*a*). At high frequencies, the kernels of wild type and most mutants fall off as f^{-4} in accordance with Eq. 3. For L15, the rolloff is more like f^{-2}, so that one of the second-order low pass filters in Eq. 3 was omitted (see below).

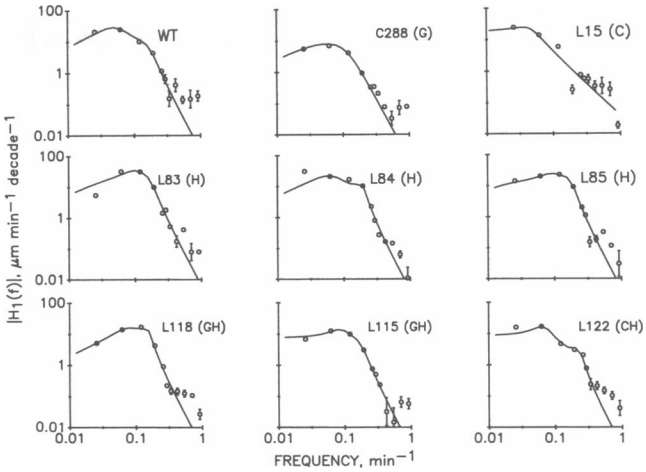

FIGURE 2 Amplitudes of complex-valued first-order kernels for wild type, and for single and double mutants affected in genes *madC*, *madG*, and *madH*. The solid lines show the results of fits of an analytical transfer function (containing two distinct low-pass filter terms for all strains but L15; see Table 3). The experimental points are shown with error bars (standard error for 6–8 experiments). For comparison, the wild-type fit is repeated as a dashed curve above all the mutant kernels.

Table 2 compares the experimental responses of wild type and the mutants. External model responses were calculated by substitution of the frequency kernels and experimental stimulus into the Wiener series. Mean-square errors (MSE) were calculated between the experimental response and the model responses up to the zero-, first- and second-order terms (Pratap et al., 1986*a*).

The response variance (MSE for the zero-order model) is smallest for C288 (G); in other words, this strain shows the weakest light-growth response. This variance is largest for L83 (H), and varies by a factor of two among different hypertropic stains. The three single hypertropic mutants have the most nonlinear light-growth response; this substantial nonlinear behavior is reflected in the consistently large percentage improvements of the second-order model response over the first-order, and in the large strengths of nonlinearity.

The first-order frequency kernels of all strains except L15 (C) were fit well by Eq. 3. The first order kernel of L15 was fit instead by the following model which lacks one of the second-order low-pass filters Poe et al., 1986*a*; Palit et al., 1986).

$$W(s) = \beta_L e^{-st_0}\left[\frac{s}{s + 2\pi f_1}\right] \cdot \left[\frac{(2\pi f_2)^2}{s^2 + (2\alpha)(2\pi f_2)\, s + (2\pi f_2)^2}\right]. \quad (5)$$

Table 3 gives the parameters estimated from the non-

TABLE 2 Experimental and model responses for wild type and mutants affected in genes *madC*, *madG*, and *madH*

Strain	Number of Experiments	Mean growth rate	MSE of response*			Percent improvement‡	Strength of nonlinearity§
			Zero order	First order	Second order		
		$\mu m\ min^{-1}$	$\mu m^2\ min^{-2}$	%	%	%	$decade^{-1}$
NRRL1555‖	7	25.9 ± 3.1	21.7	29.8	19.5	34.6	0.39
L15 (C)‖	6	34.4 ± 2.8	29.9	39.1	27.5	29.7	0.34
C288 (G)	7	36.2 ± 2.6	3.0	38.8	22.5	42.0	0.43
L83 (H)	7	34.8 ± 3.4	64.4	36.0	9.9	72.4	0.79
L84 (H)	7	26.7 ± 2.1	43.4	22.8	7.1	69.2	0.86
L85 (H)	8	35.5 ± 0.8	30.5	25.7	5.8	77.2	0.83
L122 (C H)	7	38.8 ± 2.9	21.0	47.5	21.9	53.9	0.52
L115 (G H)	7	43.6 ± 4.4	9.3	36.6	20.1	45.2	0.45
L118 (G H)	7	28.2 ± 2.4	16.7	38.8	16.2	58.3	0.43

*Mean-square errors (MSE) between experimental and external model response records (the model response was calculated by substitution of the frequency kernels and sum-of-sinusoids stimulus into the Wiener series, Pratap et al., 1986*a*). The MSE for the zero-order model (h_0) is in absolute units (note: h_0 itself is actually zero because of baseline removal; therefore, the MSE of the zero-order model is simply the variance of the response after detrending). the MSEs for first-order (h_1) and second-order (h_1 and h_2) models are given as percentages of zero-order MSE.
‡Percent improvement of second-order model over first-order model, i.e., the difference between the MSEs of the second- and first-order model responses as a percentage of the MSE of the first-order model response.
§Strength of nonlinearity is the ratio of the root-mean-square values of $|H_2(f_1, f_2)|$ and $|H_1(f)|$.
‖These results have been published earlier in Palit et. al., 1986.

linear least-squares fits of the analytical transfer function in Eq. 3 (or Eq. 5 for L15 only) to the experimental kernels. The parameters are generally similar (except to some extent f_1) for the hypertropic mutants L83 and L85, both of which carry recessive alleles of the H gene.

The absence of one of the low-pass filters in L15 can be accounted for by a shift (by mutation) of its natural frequency beyond the bandwidth (~0.11 min^{-1}) of the light-growth response (Poe et al., 1986*a*, Palit et al., 1986). However, in the double mutant L122 (CH), the natural frequency of the second low-pass filter is within the system bandwidth. The first-order high-pass filter in L15 (C) is shifted to lower frequency, below the resolution of the present set of experiments; this characteristic also appears in the double mutant L122 (CH).

Table 4 lists the parameters for the filters in the nonlinear subsystem. The hypertropic mutants L83, L84, and L85 seem to lack the low-pass filter (LP_N); i.e., the fit is better if this filter is replaced by an identity operator. The result indicates that the cutoff frequency f_{N1} has been shifted beyond the system cutoff frequency. A similar result was found for L85 at a lower log-mean intensity ($I_0 = 10^{-4}$ W m^{-2}; Palit et al., 1986).

The cutoff frequency f_{N1} for the double mutants L115

TABLE 3 First-order kernel parameters for wild type and for mutants affected in genes C, G, and H*

Strain‡	Gain factor	HPF cutoff frequency	LPF1 cutoff frequency	LPF1 damping coefficient	LPF2 cutoff frequency	LPF2 damping coefficient	Latency
	β_L $\mu m\ min^{-1}\ decade^{-1}$	f_1 min^{-1}	f_2 min^{-1}	α	f'_2 min^{-1}	α'	t_0 min
NRRL1555	40.6 ± 45.9	0.063 ± 0.095	0.052 ± 0.018	0.50 ± 0.15	0.170 ± 0.021	0.29 ± 0.09	3.3 ± 0.2
L15 (C)	19.2 ± 5.5	0.002 ± 0.009	0.045 ± 0.005	0.44 ± 0.16	—	—	3.8 ± 0.1
C288 (G)	10.5 ± 5.4	0.042 ± 0.007	0.061 ± 0.008	0.68 ± 0.10	0.132 ± 0.008	0.35 ± 0.08	3.1 ± 0.1
L83 (H)	21.0 ± 5.0	0.036 ± 0.013	0.103 ± 0.008	0.41 ± 0.13	0.168 ± 0.013	0.28 ± 0.06	3.3 ± 0.1
L84 (H)	25.9 ± 9.8	0.053 ± 0.029	0.066 ± 0.010	0.53 ± 0.08	0.193 ± 0.003	0.14 ± 0.23	3.4 ± 0.1
L85 (H)	14.2 ± 2.3	0.017 ± 0.009	0.099 ± 0.006	0.40 ± 0.10	0.179 ± 0.007	0.20 ± 0.05	3.2 ± 0.1
L122 (CH)	8.8 ± 1.5	0.000 ± 0.071	0.068 ± 0.004	0.30 ± 0.08	0.229 ± 0.010	0.14 ± 0.04	2.9 ± 0.1
L115 (GH)	7.7 ± 0.6	0.001 ± 0.005	0.091 ± 0.005	0.36 ± 0.05	0.177 ± 0.006	0.28 ± 0.05	2.8 ± 0.1
L118 (GH)	15.5 ± 7.9	0.078 ± 0.054	0.078 ± 0.012	0.45 ± 0.07	0.154 ± 0.006	0.14 ± 0.04	3.4 ± 0.1

*HPF refers to the first-order high-pass filter: LPF1, and LPF2 refer to the two low-pass filters (each of second order) in Eq. 3. For strain L15, the parameters for filter LPF2 are absent, because the fits were unsatisfactory unless this filter was excluded (see text). In all other cases, where two distinct second-order low-pass filters were used, the convention is that LPF1 has a lower cutoff frequency than LPF2 (i.e., $f_2 < f'_2$).
‡The letters in parentheses are the abbreviated *mad* genotypes. Table 1 gives the complete genotypes.

TABLE 4 Second-order kernel parameters for wild type and mutants affected in genes C, G, and H*

Strain	Gain of low-pass filter	Cutoff frequency of low-pass filter	Damping constant of low-pass filter	Gain of high-pass filter	Cutoff frequency of high-pass filter	Damping constant of high-pass filter	Exponent of high-pass filter
	β_{N1} $\text{min}^{-2}\,\text{decade}^{-1/2}$	f_{N1} min^{-1}	α_{N1}	β_{N2} $\text{min}^{-2n+1}\,\text{decade}^{-1/2}$	f_{N2} min^{-1}	α_{N2}	n
NRRL1555	0.056 ± 0.032	0.023 ± 0.002	0.97 ± 0.27	0.34 ± 0.08	0.42 ± 0.01	0.006 ± 0.011	0.32 ± 0.07
L15 (C)	0.052 ± 0.075	0.014 ± 0.012	1.18 ± 0.64	0.40 ± 0.19	0.25 ± 0.06	0.000 ± 0.012	0.51 ± 0.31
L83 (H)	—	—	—	0.74 ± 0.04	0.07 ± 0.00	0.000 ± 0.042	0.44 ± 0.02
L84 (H)	—	—	—	0.78 ± 0.05	0.07 ± 0.01	0.382 ± 0.279	0.51 ± 0.02
L85 (H)	—	—	—	0.59 ± 0.03	0.07 ± 0.00	0.015 ± 0.013	0.43 ± 0.02
C288 (G)	0.087 ± 0.044	0.028 ± 0.004	1.25 ± 0.68	0.82 ± 0.29	0.37 ± 0.03	0.268 ± 0.104	0.57 ± 0.14
L115 (GH)	0.166 ± 0.027	0.043 ± 0.002	0.94 ± 0.16	0.23 ± 0.04	0.42 ± 0.00	0.000 ± 0.000	0.23 ± 0.04
L118 (GH)	0.206 ± 0.048	0.035 ± 0.004	1.64 ± 0.40	0.26 ± 0.05	0.42 ± 0.02	0.000 ± 0.002	0.21 ± 0.05
L122 (CH)	0.074 ± 0.009	0.018 ± 0.002	1.11 ± 0.29	0.47 ± 0.08	0.31 ± 0.05	0.008 ± 0.009	0.28 ± 0.06

*The parameters were obtained by nonlinear least-squares fits of the experimental second-order kernel to the nonlinear model (Fig. 1). This model includes a dynamic nonlinear subsystem followed by a dynamic linear subsystem. The nonlinear subsystem includes a static squarer preceded by the sum of two linear filters (a low-pass filter and a high-pass filter; Eq. 4). For L83, L84, and L85, superior fits were obtained when the low-pass filter was left out. Therefore only the parameters of the high-pass filter in the nonlinear subsystem is shown.

and L118 (GH) is intermediate between the values for the G and H single mutants. The phenotypes of GH double mutants tend to be intermediate between the parental phenotypes (López-Díaz and Lipson, 1983). The cutoff frequency f_{N2} of L115 and L118 (GH) is similar to that of G and the wild type. In the double mutant L122 (CH), f_{N2} is approximately the same as in wild type and higher than in either parental. A mutation in C or G along with one in H tends to restore f_{N2} to the wild-type value.

The damping factors α_{N1} and α_{N2} do not vary significantly among the single or double mutants tested. The exponent n in all the double mutants is ~0.25, which is approximately half of the values in the single mutants and wild type (~0.5).

Interaction tests

If two components (gene products) of the sensory system act independently in cascade, then one can derive the following relations for the kernels of the respective single mutants, double mutant and wild type (Palit, 1987). Let $K_1(f)$ and $K_2(f_1,f_2)$ denote the first- and second-order frequency kernels of wild type. Similarly, let K_1^c, K_1^g, and K_1^h, and K_2^c, K_2^g, and K_2^h denote the corresponding kernels for the C, G, and H mutants. If, for example, the C and H gene products act in sequence (cascade) as independent (noninteracting) components in the sensory pathway, then:

$$K_1^{ch}(f) \cdot K_1(f) = K_1^c(f) \cdot K_1^h(f) \quad (6)$$

$$K_2^{ch}(f_1,f_2) \cdot K_2(f_1,f_2) = K_2^c(f_1,f_2) \cdot K_2^h(f_1,f_2), \quad (7)$$

where K_1^{ch} and K_2^{ch} are the kernels of the CH double mutant.

To test the null hypothesis (i.e., no interaction), the following ratios of the complex-valued kernels were evaluated:

$$Q_1 = \frac{K_1^{ch}(f) \cdot K_1(f)}{K_1^c(f) \cdot K_1^h(f)} \quad (8)$$

$$Q_2 = \frac{K_2^{ch}(f_1,f_2) \cdot K_2(f_1,f_2)}{K_2^c(f_1,f_2) \cdot K_2^h(f_1,f_2)}. \quad (9)$$

According to Eqs. 6 and 7, one would require $Q_1 = 1$ and $Q_2 = 1$. However, because the overall magnitudes of the kernels depend to some extent on the average growth velocity of the sporangiophore, we have relaxed this condition slightly, and require only that Q_1 and Q_2 be real constants. Thus Q_1 and Q_2 should not depend significantly on frequency, nor should the phases of Q_1 and Q_2 differ significantly from zero.

Table 5 shows the results of such tests of Eqs. 8 and 9 applied to the kernels for the double mutants, single mutants and wild type in each combination. Two criteria are applied to evaluate the least-square fits: (*a*) the goodness of fit according to the normalized chi-square, and (*b*) the requirement that Q_1 and Q_2 be real.

The stimulus used to probe the system was a sum of 15 sinusoids, so there are 15 first-order complex-valued frequency points. The second-order kernel points are obtained from the Fourier transforms of the response at the combination frequencies (sums and differences of the component frequencies). We therefore get 15^2 (equals 225) second-order kernel points from the experimental data.

Each of the complex-valued constants Q_1 or Q_2 (Eqs. 8 and 9) includes two real numbers (real and imaginary parts). Therefore, the number of degrees of freedom

TABLE 5 **Interaction tests for gene pairs CH and GH***

Gene pair tested‡	First order (linear)			Second order (nonlinear)		
	$\|Q_1\|$	$/Q_1$	Goodness-of-fit parameter for Q_1	$\|Q_2\|$	$/Q_2$	Goodness-of-fit parameter for Q_2
CH (L122)	0.52 ± 0.09	12.6 ± 11.6	1.73	0.20 ± 0.01	−16.7 ± 2.0	5.22
GH (L115)	1.26 ± 0.16	−3.6 ± 7.2	0.67	0.28 ± 0.02	5.6 ± 5.1	1.28
GH (L118)	1.28 ± 0.17	4.3 ± 7.7	0.57	0.26 ± 0.03	19.4 ± 16.3	1.25

*The error-weighted average of Q_1 was evaluated for the 15 component frequencies (i.e., the 15 values of Q_1 were fit in effect to a constant), and similarly for Q_2 at the 225 combination frequencies. The third and fourth columns give the magnitude and phase of the average Q_1 (and similarly sixth and seventh column for Q_2). The goodness-of-fit parameter is the normalized chi-square (error-weighted sum of squares of residuals). The null hypothesis (no interaction) can be rejected at the 5% significance level if either (*a*) the phase of Q_1 (or Q_2) differs from zero by more than 1.96 times the tabulated standard error, or (*b*) the goodness-of-fit parameter exceeds 1.48 for Q_1 or 1.11 for Q_2 (values obtained from a chi-square table). The values for which the null hypothesis fails are underlined.

‡The double mutants used in the tests are indicated in parentheses.

(number of data points minus number of parameters) is 28 (equals 30 − 2) for the first-order analysis and 448 (equals 450 − 2) for the second-order analysis. The normalized chi-square (i.e., chi-square divided by the number of degrees of freedom) is used as a goodness-of-fit parameter. At the 5% significance level, with 28 degrees of freedom, a model can be rejected if the normalized chi-square exceeds 1.48. Similarly, for 448 degrees of freedom (second-that order analysis), the critical value for the normalized chi-square is 1.11. For Q_1 and Q_2 to be real, the criterion for rejecting the hypothesis at the 5% significance level is that the phase angle should deviate from zero by more than 1.96 times the standard error.

From both the first- and second-order analyses, the CH double mutant fails the cascade hypothesis. The phases of Q_1 and Q_2 are nonzero for the second-order analysis, and the normalized chi-square values for both the first- and second-order analyses (1.73 and 5.22 respectively) exceed the critical values (1.48 and 1.11).

For the two GH double mutants (L115 and L118) the phases of Q_1 and Q_2 do not differ significantly from zero. The normalized chi-square values for the first-order analysis are <1.48, but for the second-order analysis the values are >1.11. Therefore, the GH gene pair fails to satisfy the null hypothesis of no interaction for the second-order analysis only.

DISCUSSION

Parametric analysis

We have analyzed the first- and second-order kernels in terms of the model (Fig. 1) introduced by Pratap et al. (1986*a*). It includes a linear dynamic subsystem preceded by a nonlinear subsystem; the latter consists of linear dynamic elements (low-pass and high-pass filters) and a static squarer. The linear subsystem includes two low-pass filters, a high-pass filter, a delay element, and a gain term.

The nonlinear least-squares fits of the external model response to the experimental response provided estimates of the parameters in the internal model (Tables 3 and 4). The similarity between the first-order kernels of the GH double mutants and of the G single mutant is consistent with the finding that the H mutation affects only the nonlinear subsystem of the model (Palit et al., 1986).

In the H mutants, the low-pass filter in the nonlinear subsystem seems to be absent. Furthermore, the C mutant behaves as if it lacks one of the second-order low-pass filters in the linear subsystem. It was hypothesized (Palit et al., 1986) that these filters are absent because their cutoff frequencies were shifted beyond the system bandwidth (i.e., in the C mutant, these steps proceed significantly faster than the rate-limiting step(s) of the entire system). However, in the GH double mutant, the low-pass filter of the nonlinear subsystem is present, but has a higher cutoff frequency than that of G mutant. Similarly in the linear subsystem, the low-pass filter cutoff frequency of the double mutant L122 (CH) exceeds that of the hypertropic mutant L85. Therefore, the double mutants have characteristics intermediate between those of their parentals.

Interaction tests

The lack of complementation between C and H mutations at high light intensity (10 W m^{-2}) suggested that the C and H gene products interact under these conditions (López-Díaz and Lipson, 1983). From our experiments, which were performed at a log-mean intensity I_0 of 6×10^{-2} W m^{-2}, the double mutant L122 fails the cascade hypothesis. The gene products of C and H evidently

interact at these lower intensities also (at least for the light-growth response).

We have tested two GH double mutants. L115 carries a dominant allele of H and L118 carries a recessive allele. The conclusions from both mutants are generally similar. Therefore, for the hypertropic strains tested, the results of the interaction tests do not appear to be allele specific.

The tests with the first-order kernel revealed no significant interaction between the products of genes G and H. The phase of Q_1 is within 1.96 standard errors of zero, and the value of the normalized chi-square is <1.48 (the critical value for the first-order analysis, at the 5% significant level). When the second-order kernel was used to determine the dynamic interaction, we found that the phase of Q_2 again does not differ significantly from zero, but the normalized chi-square exceeds 1.13 (critical value for second-order analysis). Therefore the null hypothesis that there is no interaction between gene products fails for the second-order analysis. Our results indicate that the G and H gene products interact in the nonlinear subsystem rather than in the linear subsystem. The results suggest that the G and H gene products are weakly coupled components of the sensory transduction complex. Such components would interact only when the system is driven with large stimuli, large enough to drive nonlinear responses.

The hypertropic mutants were isolated for their enhanced tropisms (Lipson et al., 1983). From the altered photogravitropic action spectrum of a hypertropic mutant, it was concluded that the mutation affects not only the growth control output of the sensory transduction system for phototropism and light-growth response, but also the photoreceptor input (Galland and Lipson, 1985). To explain how a single mutation could affect both the input and output of a system, it was assumed that there is an integrated sensory tranduction complex (instead of a sequential chain of transducers) that manages not only photoresponses but also other responses like gravitropism and avoidance (Palit et al., 1986). Extensive interactions found between the input gene products (A, B, C) and the output gene products (D, E, F, and G) supported this hypothesis (Poe et al., 1986*b*).

Our results provide further support. The night-blind (C) mutant is associated with the photoreceptor input of the photosensory transduction complex and most probably is a photoreceptor mutant (Galland and Lipson, 1985). The stiff (G) mutant is associated with the growth control output of the sensory tranduction complex. From the results of the interaction analysis we find that the H gene product interacts with both the C and the G gene products. The results with double mutants carrying hypertropic mutations thus confirm and extend the previous findings that hypertropic mutations affect both the input and the output of the light-growth response system (Palit et al., 1986). The results provide additional support for the existence of an integrated sensory transduction complex managing the light-growth response as well as other behavioral responses of the *Phycomyces* sporangiophore.

This work was supported by grant GM29707 from the National Institutes of Health to Edward D. Lipson.

Received for publication 13 September 1988 and in final form 17 November 1988.

REFERENCES

Cerdá-Olmedo, E., and E. Lipson. 1987. *Phycomyces*. Cold Spring Harbor Laboratory, Cold Spring Harbor, NY.

Foster, K. W., and E. D. Lipson. 1973. The light growth response of *Phycomyces*. *J. Gen. Physiol.* 62:590–617.

Galland, P., and E. D. Lipson. 1985. Modified action spectra of photogeotropic equilibrium in *Phycomyces blakesleeanus* mutants with defects in genes *madA*, *madB*, *madC*, and *madH*. *Photochem. Photobiol.* 41:331–335

Hamilton, W. C. 1964. Estimation, hypothesis testing, and least squares. *In* Statistics in Physical Science. The Ronald Press Company, New York.

Lipson, E. D. 1975*a*. White noise analysis of *Phycomyces* light growth response system. I. Normal intensity range. *Biophys. J.* 15:989–1012.

Lipson, E. D. 1975*b*. White noise analysis of *Phycomyces* light growth response system. II. Extended intensity ranges. *Biophys. J.* 15:1013–1032.

Lipson, E. D. 1975*c*. White noise analysis of *Phycomyces* light growth response system. III. Photomutants. *Biophys. J.* 15:1033–1045.

Lipson, E. D., I. López-Díaz, and J. A. Pollock. 1983. Mutants of *Phycomyces* with enhanced tripoisms. *Exp. Mycol.* 7:241–252.

Lopez-Díaz, I., and E. D. Lipson. 1983. Genetic analysis of hypertropic mutants of *Phycomyces*. *Mol. Gen. Genet.* 190:318–325.

Marmarelis, P., and V. Z. Marmarelis. 1978. Analysis of physiological systems. The white-noise approach. Plenum Publishing Corp., New York.

Marquardt, D. W. 1963. An algorithm for least-squares estimation of nonlinear parameters. *J. Soc. Indust. Appl. Math.* 11:431–441.

Palit, A. 1987. Nonlinear system analysis of light-growth response in behavioral mutants of *Phycomyces*. Ph.D. Dissertation, Syracuse University, Syracuse, NY. 72–74.

Palit, A., P. Pratap, and E. D. Lipson. 1986. System analysis of *Phycomyces* light-growth response: photoreceptor and hypertropic mutants. *Biophys. J.* 50:661–668.

Poe, R. C., and E. D. Lipson. 1986. System analysis of *Phycomyces* light-growth response with Gaussian white noise test stimuli. *Biol. Cybern.* 55:91–98.

Poe, R. C., P. Pratap, and E. D. Lipson, 1986*a*. System analysis of *Phycomyces* light-growth response: single mutants. *Biol. Cybern.* 55:99–104.

Poe, R. C., P. Pratap, and E. D. Lipson. 1986*b*. System analysis of *Phycomyces* light-growth response: double mutants. *Biol. Cybern.* 55:105–113.

Pratap, P., A. Palit, and E. D. Lipson. 1986*a*. System analysis of *Phycomyces* light-growth response with sum-of-sinusoids test stimuli. *Biophys. J.* 50:645–651.

Pratap, P., A. Palit, and E. D. Lipson. 1986*b*. System analysis of *Phycomyces* light-growth response: wavelength and temperature dependence. *Biophys. J.* 50:653–660.

Stanley, W. D. 1975. Digital Signal Processing. Reston Publishing Co., Reston, VA, 256–273.

Victor, J. D., and R. M. Shapley. 1980. A method of nonlinear analysis in the frequency domain. *Biophys. J.* 29:459–484.